Functional analysis of an individual IFT protein: IFT46 is required for transport of outer dynein arms into flagella

Yuqing Hou,[1] Hongmin Qin,[3] John A. Follit,[2] Gregory J. Pazour,[2] Joel L. Rosenbaum,[3] and George B. Witman[1]

[1]Department of Cell Biology and [2]Program in Molecular Medicine, University of Massachusetts Medical School, Worcester, MA 01655
[3]Department of Molecular, Cellular, and Developmental Biology, Yale University, New Haven, CT 06520

Intraflagellar transport (IFT), which is the bidirectional movement of particles within flagella, is required for flagellar assembly. IFT particles are composed of ~16 proteins, which are organized into complexes A and B. We have cloned *Chlamydomonas reinhardtii* and mouse *IFT46*, and show that IFT46 is a highly conserved complex B protein in both organisms. A *C. reinhardtii* insertional mutant null for IFT46 has short, paralyzed flagella lacking dynein arms and with central pair defects. The mutant has greatly reduced levels of most complex B proteins, indicating that IFT46 is necessary for complex B stability. A partial suppressor mutation restores flagellar length to the *ift46* mutant. IFT46 is still absent, but levels of the other IFT particle proteins are largely restored, indicating that complex B is stabilized in the suppressed strain. Axonemal ultrastructure is restored, except that the outer arms are still missing, although outer arm subunits are present in the cytoplasm. Thus, IFT46 is specifically required for transporting outer arms into the flagellum.

Introduction

Intraflagellar transport (IFT) is the bidirectional movement of granule-like particles, termed IFT particles, along the length of eukaryotic cilia and flagella (Rosenbaum and Witman, 2002; Scholey, 2003). IFT was first reported in the green alga *Chlamydomonas reinhardtii* (Kozminski et al., 1993), and has subsequently proven to be a conserved process among ciliated organisms (Cole et al., 1998). IFT moves axonemal components, such as cargo, to the tip of the flagellum (Piperno and Mead, 1997; Qin et al., 2004), where axonemal assembly occurs (Witman, 1975; Johnson and Rosenbaum, 1992). IFT is also involved in the turnover of flagellar components (Qin et al., 2004), in the movement of flagellar membrane components in the plane of the membrane (Qin et al., 2005), and in cilium-generated signaling (Wang et al., 2006). Consequently, mutations in IFT affect ciliary and flagellar assembly, maintenance, and function (Rosenbaum and Witman, 2002; Scholey, 2003; Pan et al., 2005).

Considerable progress has been made in understanding the structure and composition of the IFT particles and the motors that move them. IFT from the base to the tip of the flagellum is powered by kinesin-2 motors (Kozminski et al., 1995; Snow et al., 2004); IFT in the opposite direction is generated by cytoplasmic dynein 1b (Pazour et al., 1998, 1999; Porter et al., 1999; Signor et al., 1999). The IFT particles themselves are composed of at least 16 proteins organized into two complexes, complexes A and B (Table I; Cole, 2003), which sediment at 16S in sucrose density gradients. Biochemical analysis has revealed that complex B contains an ~500-kD core composed of IFT88, IFT81, IFT74/72, IFT52, IFT46, and IFT27 (Lucker et al., 2005). IFT172 appears to be a peripheral component, as it often dissociates from complex B during the latter's purification (Cole et al., 1998).

Much less is known about the functions of the individual IFT particle proteins, and how they interact with the IFT cargoes. Many of the *C. reinhardtii* IFT particle proteins have been sequenced, but the sequences provide few hints as to the proteins' functions. Recognizable domains consist mainly of WD repeats, TPR domains, and coiled-coil domains, all of which are thought to be involved in protein–protein interactions (Cole, 2003). Mutations have been identified for *C. reinhardtii* IFT52, IFT88, and IFT172, but these generally block flagellar assembly (Huang et al., 1977; Pazour et al., 2000; Brazelton et al., 2001; Pedersen et al., 2005), and thus have not been informative in regard to the proteins' specific functions. Mutations in genes encoding IFT proteins in *Caenorhabditis elegans* and mammals have been similarly uninformative (Perkins et al., 1986; Pazour et al., 2000).

Correspondence to George Witman: george.witman@umassmed.edu
Abbreviation used in this paper: IFT, intraflagellar transport.
The online version of this article contains supplemental material.

The Journal of Cell Biology, Vol. 176, No. 5, February 26, 2007 653–665
http://www.jcb.org/cgi/doi/10.1083/jcb.200608041

Table I. ***C. reinhardtii*** **IFT particle proteins**

Complex A	Complex B
IFT144	IFT172
IFT140	IFT88
IFT139	IFT81
IFT122A	IFT80
IFT122B	IFT74/72
IFT43	IFT57/55
	IFT52
	IFT46
	IFT27
	IFT20

In *C. reinhardtii*, IFT172 interacts with EB1, which is located at the tip of the flagellum (Pedersen et al., 2003, 2005), and an IFT172 temperature-sensitive mutant is defective in IFT particle turnaround at the tip of the flagellum (Pedersen et al., 2005); based on these results, it was proposed that IFT172 is involved in regulating the transition between anterograde and retrograde IFT (Pedersen et al., 2005). In mammalian cells, IFT20 was found to be unique among IFT particle proteins examined in that it is localized to the Golgi apparatus, as well as the cilium, and moderate knockdown of IFT20 reduced the amount of the membrane protein polycystin-2 in the cilium (Follit et al., 2006), suggesting that IFT20 is involved in trafficking of ciliary membrane proteins. Other than this, nothing is known about the specific roles of the IFT particle proteins and how, or even whether, they interact with specific cargoes.

To obtain more information on the function of a specific IFT particle protein, we have focused on IFT46, which was previously briefly reported to be a complex B protein in *C. reinhardtii* (Cole et al., 1998). We have cloned and characterized IFT46 from *C. reinhardtii* and mouse, and find that it is a homologue of DYF-6, a protein very recently reported to undergo IFT in *Caenorhabditis elegans* and to result in truncated dendritic cilia when mutated in the worm (Bell et al., 2006). We also describe the phenotype of a *C. reinhardtii*-null mutant for IFT46, and of a suppressor of that mutant. The observations provide new insights into the role of IFT46 in IFT particle stability and transport of a specific IFT cargo. Portions of this work were previously reported in abstract form (Hou et al., 2005).

Results

Cloning of *C. reinhardtii* IFT46

The gene and cDNA encoding *C. reinhardtii* IFT46 were cloned as described in Materials and methods. The cDNA (accession no. DQ787426) contains a 1,035-nt ORF predicted to encode a 37.9-kD protein (Fig. 1 A) with a pI of 4.61. The cDNA has a stop codon 18 nt upstream of the predicted start codon, and a polyA consensus sequence at nt 1,703–1,707. ESTs have a polyA tail 12–14 nt downstream of the polyA consensus sequence. Therefore, the ORF is complete. No structural domains or motifs were identified within the sequence.

IFT46 was initially identified as an IFT complex B protein, based on its cosedimentation with other complex B proteins

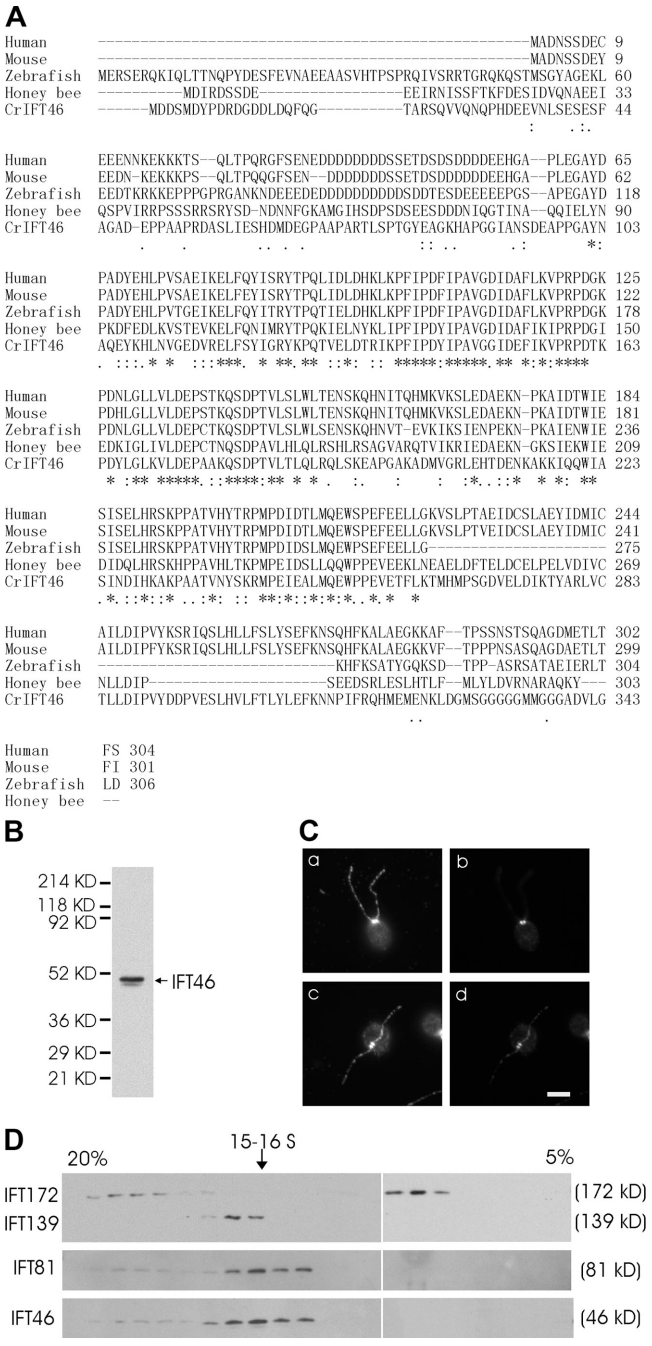

Figure 1. **Identification and characterization of *C. reinhardtii* IFT46.** (A) Predicted amino acid sequence of IFT46 and alignment with orthologues from other organisms. CrIFT46 is highly conserved from aa 100–315. Amino acid identities are marked with asterisks; similarities are marked with either one or two dots. Sequences used in this alignment are as follows: human (AAH22856), mouse (NP_076320), zebrafish (XP_694278), honey bee (XP_396519), and CrIFT46 (DQ787426). (B) The antibody to IFT46 specifically recognizes a ~46-kD doublet in Western blots of whole cell lysates; the doublet is caused by phosphorylation (unpublished data). (C) IFT46 has a typical cellular localization for an IFT particle protein. Cells were labeled with the anti-IFT46 antibody. Images of the same cell were acquired focusing at the flagella (a and c), or at the basal body region (b and d) with much less exposure time. The majority of IFT46 is located at the peribasal body region, with a lesser amount distributed along the flagella as distinct dots. Bar, 5 μm. (D) IFT46 comigrates with IFT81, an IFT complex B protein, in sucrose gradients. The flagellar membrane plus matrix was fractionated in a 5–20% sucrose gradient. The fractions were analyzed by Western blotting using antibodies to IFT46, complex B proteins IFT172 and IFT81, and complex A protein IFT139. Under these experimental conditions, complex B separated from complex A, and IFT172 dissociated from complex B.

in sucrose gradients (Cole et al., 1998). Characterization of our cloned protein indicates that it behaves exactly as expected of a 46-kD complex B protein, as follows: a) six unique peptides corresponding to the cloned protein were identified in the membrane plus matrix fraction of the flagellar proteome, but no peptides from it were found in any other fraction, which is a distribution typical for IFT particle proteins but unusual for non-IFT proteins (Pazour et al., 2005); b) using real-time PCR, we found that expression of the protein is up-regulated 10.4 ± 2.03-fold (SEM) upon deflagellation, which is characteristic of flagellar proteins, including other complex B proteins (Pazour et al., 2005); c) an antibody to a peptide contained in the cloned protein was generated and shown to react specifically with a single protein of M_r ~46,000 in Western blots of whole cell lysates (Fig. 1 B); d) immunofluorescence microscopy with the antibody as probe showed that the majority of the cloned protein is located in the basal body region, with a lesser amount in puncta along the length of the flagella (Fig. 1 C), is a distribution identical to that of other IFT particle proteins (Cole et al., 1998; Deane et al., 2001); moreover, the protein colocalized with complex B protein IFT172, but not complex A protein IFT139 (see the section Complex A and B proteins are located in distinct compartments in the basal body region; Fig. 6 B); and e) when the flagellar membrane plus matrix fraction was analyzed by sucrose density gradient centrifugation, the cloned protein co-migrated precisely with IFT81, a complex B protein, but not with IFT139, a complex A protein (Fig. 1 D). These results indicate that the cloned protein is indeed IFT46, and confirm that IFT46 is a complex B protein.

IFT46 is highly conserved

Database searches revealed that IFT46 is conserved across organisms that have cilia, including *Danio rerio* (XP_694278; BLAST E, 1e-47), *Apis melifera* (XP_396519; BLAST E, 1e-47), *Drosophila melanogaster* (NP_609890; BLAST E, 1e-17), *Mus musculus* (NP_076320; BLAST E, 2e-61), and *Homo sapiens* (CAB66868; BLAST E, 8e-62). The protein is also homologous to *C. elegans* DYF-6 (NP_741887; BLAST E, 9e-34), which was recently reported to undergo IFT in dendritic cilia when fused to GFP (Bell et al., 2006). No similar sequence was found in nonciliated organisms, including *Saccharomyces cerevisiae* and *Arabidopsis thaliana*.

The middle portions of the *C. reinhardtii* and mammalian proteins are highly similar (51% identity, 72% similarity; Fig. 1 A), making it likely that they are orthologous proteins. To test this, the putative mouse orthologue was Flag tagged and expressed in IMCD3 cells, a mouse kidney cell line. Immunofluorescence microscopy revealed that the Flag-tagged protein localized specifically to primary cilia (Fig. 2 A). To determine if the mammalian protein was part of IFT complex B, lysates were prepared from IMCD3 cells expressing either IFT46-Flag, IFT20-Flag (positive control), or GFP-Flag (negative control) and immunoprecipitated with an anti-Flag antibody. In each case, the Flag-tagged proteins were highly enriched in the immunoprecipitates (Fig. 2 B, top). Western blots showed that complex B proteins IFT88 and IFT57, but not complex A protein IFT140 or a control protein, were coimmunoprecipitated from lysates of the IFT46-Flag–expressing cells (Fig. 2 B, bottom). Similarly, in the positive control, IFT88 and IFT57, but not IFT140, were coimmunoprecipitated. No IFT proteins were coimmunoprecipitated from the lysate of cells expressing GFP-Flag. Therefore, mammalian IFT46 localizes to cilia and is tightly associated with complex B proteins, but not with complex A proteins.

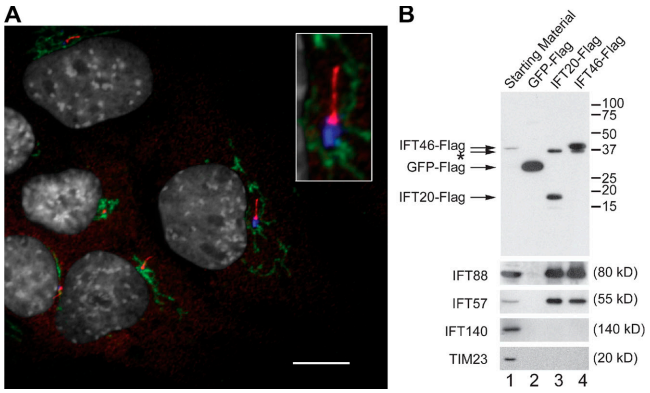

Figure 2. **The mouse orthologue of CrIFT46 is also an IFT complex B protein.** (A) MmIFT46 localizes in cilia. IMCD3 cells expressing Flag-tagged MmIFT46 were labeled with antibodies to Flag (red), IFT20 (green), which localizes to Golgi in addition to cilia, and a centrosome component (blue). Nuclei were DAPI stained and are shown as gray. IFT46-Flag was concentrated at the bases of the cilia, but was also located along the length of the cilia. The inset shows an enlargement of one of the cilia. Bar, 10 μm. (B) IFT complex B proteins coimmunoprecipitate with MmIFT46. Whole-cell lysates from mouse IMCD3 cells expressing Flag-tagged GFP (lane 2), Flag-tagged IFT20 (lane 3), or Flag-tagged IFT46 (lane 4) were immunoprecipitated with an anti-Flag antibody. The immunoprecipates were analyzed by Western blotting with antibodies to Flag (top), IFT88, IFT57, IFT140, and TIM23, which is a mitochondrial protein used as a control (bottom). (top) The positions of the Flag-tagged proteins are indicated with arrows. *, an irrelevant protein that is recognized by the Flag antibody. Lane 1 is the starting material for the IFT46-Flag immunoprecipitation. Note that IFT46-Flag is highly enriched by the immunoprecipitation (compare lanes 1 and 4). Lanes were loaded with equivalent amounts of protein, except that in the top gel only, lane 2 was loaded with 1/50 the amount of protein that is present in the other lanes. Complex B proteins IFT88 and IFT57 coimmunoprecipitated with MmIFT46-FLAG (and MmIFT20-FLAG), whereas complex A protein IFT140 and TIM23 did not, even though they were present in the starting material. No IFT proteins were coimmunoprecipated from the lysate of the Flag-GFP–expressing cells.

IFT46 is necessary for flagellar assembly

To investigate the role of IFT46 in intraflagellar transport, we screened a collection of *C. reinhardtii* insertional mutants by Southern blotting and identified one strain, T8a44-11, with a defect in the *IFT46* gene. Analysis by PCR showed that the mutant allele, which we term *ift46-1*, has a deletion or disruption somewhere between the fourth and the seventh exon of the *IFT46* gene (Fig. 3, A and B). This mutant has short, stumpy flagella.

Strain T8a44-11 was backcrossed to wild-type cells, and a progeny, YH6, which lacked the *pf1* mutation carried by the parental strain, was selected for detailed characterization. As in T8a44-11, the *IFT46* gene in YH6 is disrupted, as shown by Southern blotting (Fig. 3 C, lane 2). No IFT46 can be detected in lysates of YH6 cells (Fig. 3 D, lane 2), indicating that IFT46 is not expressed in YH6 cells. Thus, the mutant allele is a null allele (see also the section The 3′ end of the *IFT46* gene is

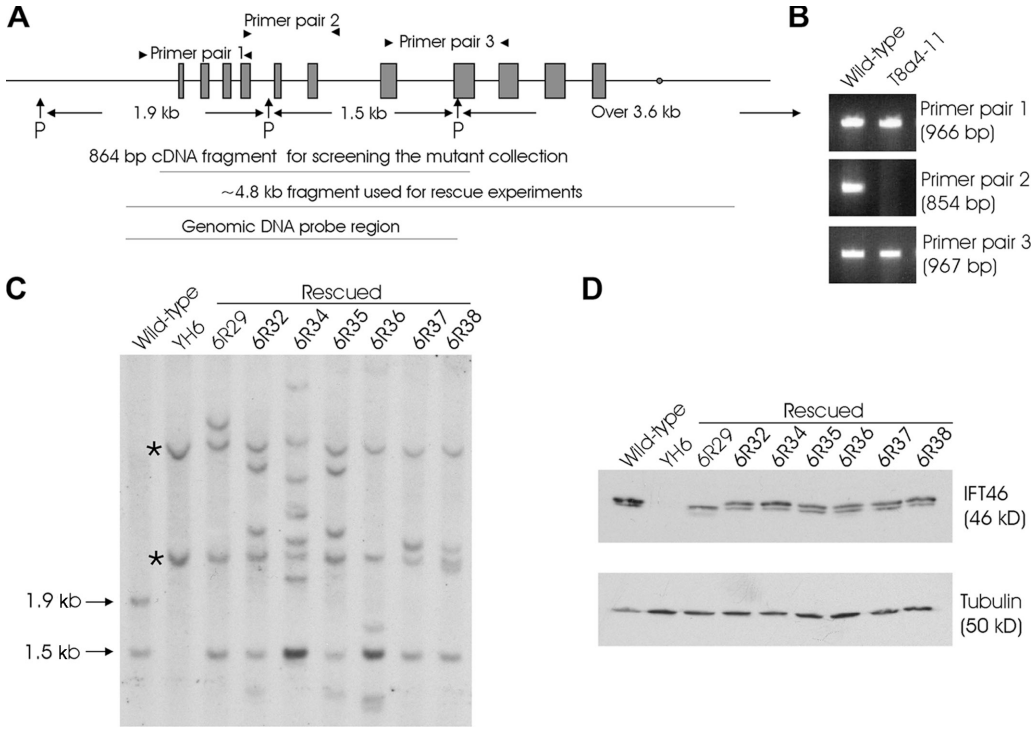

Figure 3. **The nonmotile phenotype of YH6 is caused by a null mutation in the *IFT46* gene.** (A) *IFT46* gene structure. There are two PstI sites (P) within the *IFT46* gene. Three primer sets used for PCR to map the mutation region in the mutant are indicated by arrowheads. Regions corresponding to the ~4.8-kb genomic fragment used for rescue experiments, the cDNA probe used for screening the mutant collection, and the genomic DNA probe used for Southern blotting also are shown. (B) PCR results using primers to different regions of the *IFT46* gene showed that strain T8a4-11 is defective in the middle portion of the gene. (C and D) The nonmotile phenotype of YH6, which is an offspring of a cross between T8a4-11 and wild-type cells, was rescued by transforming the mutant cells with the wild-type *IFT46* gene. Genomic DNAs from wild-type cells, YH6, and rescued cells were cut by PstI and analyzed by Southern blotting using a *IFT46* genomic DNA probe (C). The rescued cells (6R29 through 6R38) have the 1.5-kb fragment originating from the transgene (the 1.9-kb fragment is missing because it was not present in its entirety in the transgene) and two hybridizing bands (*) originating from the mutated *ift46* gene. They also have other hybridizing bands, indicating that the *IFT46* transgenes were incorporated at different sites. Western blots of whole cell lysates (D) show that YH6 cells lack the IFT46 protein and that the rescued cells express IFT46 protein. The same blot was stripped and probed with an anti-tubulin antibody as control (bottom).

transcribed in $Sup_{ift46}1$ cells). Like T8a44-11, YH6 cells have short, stumpy flagella that barely extend beyond the flagellar collar (Fig. 4). The flagella are nonmotile.

To confirm that the mutant phenotype of YH6 was caused by the disruption of the *IFT46* gene, YH6 cells were transformed with a 4.8-kb fragment containing only the wild-type *IFT46* gene (Fig. 3 A). Numerous wild-type swimmers with full-length flagella were recovered. Southern blotting revealed that the exogenous *IFT46* gene had integrated into the genome at different sites in several of these rescued strains (Fig. 3 C, lanes 3–9), confirming that the rescued strains were independently derived. Therefore, restoration of motility was caused by incorporation of the transgene, and not caused by disruption of some other gene. Western blotting confirmed that expression of IFT46 was restored in the transformants (Fig. 3 D, lanes 3–9). These results demonstrate that the short flagella phenotype of YH6 is caused by the absence of IFT46. Hereafter, this strain will be referred to as the *ift46* mutant.

The *ift46* mutant has unique defects in its axoneme

Although very short, *ift46* flagella are longer than those of mutants with defects in the complex B proteins IFT88 (Pazour et al., 2000) and IFT52 (Brazelton et al., 2001), which do not form flagella beyond the transition region. Because flagella are formed in the *ift46* mutant, we were able to compare them with flagella from wild-type and rescued cells by EM to identify flagellar defects associated with loss of IFT46. Serial sections of wild-type flagella have shown that the outer doublet microtubules are connected by rodlike "peripheral links" in the most proximal part of the flagella (Fig. 4 A, a); the rows of dynein arms begin at a level slightly more distal, but still within the flagellar collar (Fig. 4 A, b; Hoops and Witman, 1983). The *ift46* flagella have nine outer doublet microtubules and frequently extend to the limits of the flagellar collar or beyond (Fig. 4 A, f–p), but we never observed dynein arms in longitudinal or cross sections of these axonemes. In addition, the mutant flagella lack the projections into the lumens of the B-tubule (Hoops and Witman, 1983) and frequently have defects in the central pair of microtubules (Fig. 4 A, f–k). In contrast to mutants with defects in the retrograde IFT motor (Pazour et al., 1999; Porter et al., 1999; Hou et al., 2004), few, if any, IFT particles accumulate in the *ift46* mutant flagella. It is important to note that the flagella from the rescued cells (Fig. 4 A, d and e) have typical wild-type morphology with normal inner and outer dynein arms and central pair microtubules; this confirms that

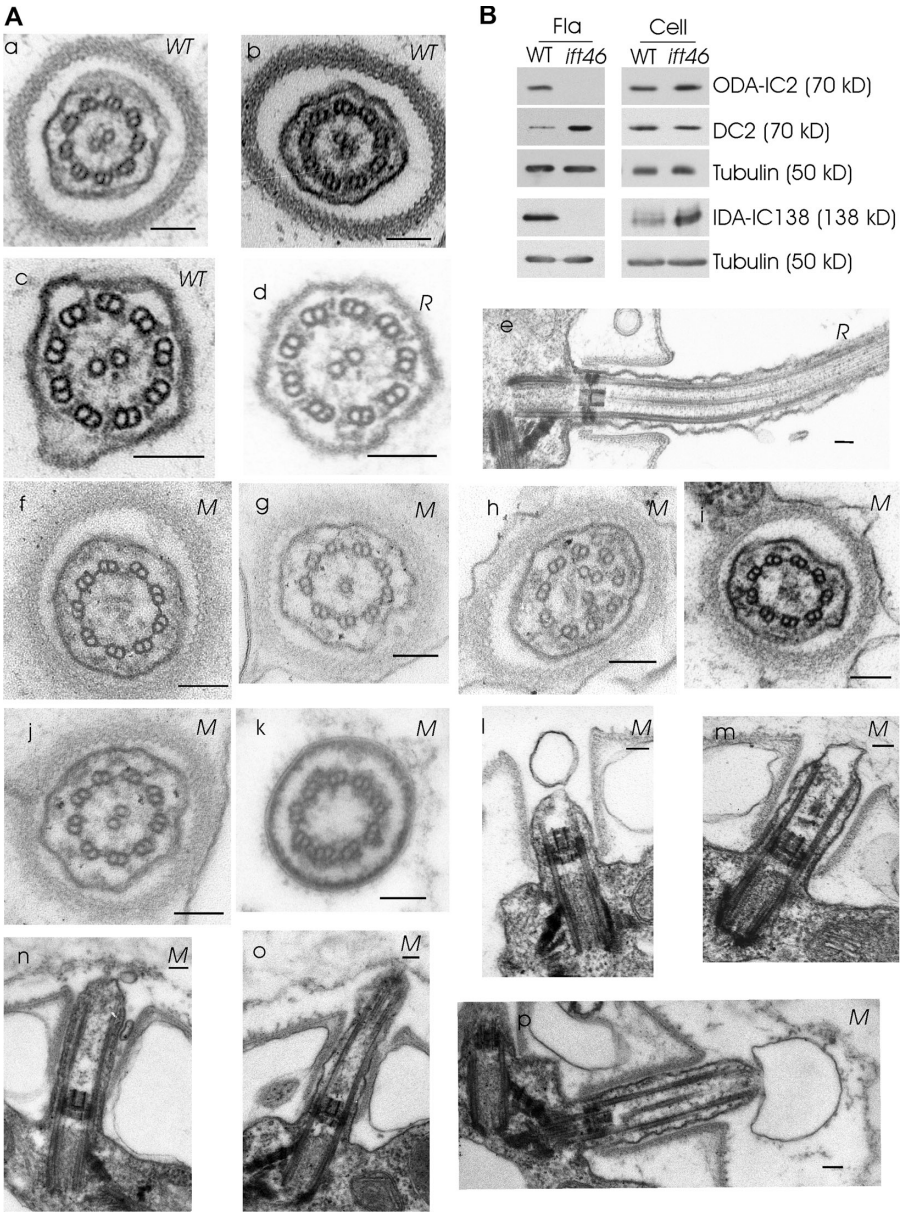

Figure 4. **Flagellar assembly is defective in *ift46* mutant cells.** (A) Electron micrographs show that *ift46* flagella are short with normal basal bodies and transition zones. The mutant flagella lack dynein arms, and central pair assembly is defective. (a–c) Cross sections of wild-type (*WT*) flagella. (d) Cross section of a flagellum of the rescued cell line 6R32 (*R*). (e) Longitudinal section of a flagellum of 6R32. (f–k) Cross sections of *ift46* flagella (*M*). (l–p) Longitudinal sections of *ift46* flagella (*M*). The membrane vesicles or bulges frequently present at the tips of the short mutant flagella are also observed in the *ift88* mutant (Pazour et al., 2000). Bars, 100 nm. (B) Western blotting shows that *ift46* flagella lack outer dynein arm and inner dynein arm components, although these components exist in the cell cytoplasm. In contrast, the outer dynein arm docking complex is transported into *ift46* flagella. Flagellar samples (Fla) and whole cell lysates (Cell) from *ift46* or wild-type cells were probed with antibodies to IC2 (an outer dynein arm component), IC138 (an inner dynein arm I1 component), or DC2 (a subunit of the outer dynein arm docking complex). Tubulin was probed as a loading control.

the ultrastructural defects seen in the mutant are caused by loss of IFT46.

To determine whether the dynein arm deficiency in the *ift46* mutant is caused by degradation of dyneins within the cell body, by an inability to transport dyneins into the flagella, or by an inability to assemble them onto the axonemes, we analyzed whole cell lysates and flagella from *ift46* and wild-type cells by Western blotting (Fig. 4 B). The cell lysates of the mutant contained normal levels of the outer arm dynein intermediate chain IC2 and the inner arm dynein intermediate chain IC138. Therefore, the dyneins are present in the mutant cells. However, both IC2 and IC138 were completely absent from the *ift46* mutant flagella, indicating that the dyneins are not transported into the flagella. In contrast, DC2, which is a component of the outer dynein arm docking complex that is transported into the wild-type flagellum and assembled onto the doublets independently of the outer dynein arm (Wakabayashi et al., 2001), is transported into the *ift46* flagella. The presence of DC2 in the flagella provides additional evidence that the lack of dynein arms is not simply because of the short length of the mutant flagella or to a general failure to transport proteins into the flagellum. These data confirm that the ultrastructural findings that the *ift46* mutant has a defect in transporting dynein arms into the flagella.

IFT complex B is unstable in the absence of IFT46

To investigate the role of IFT46 in IFT complex assembly, we examined the cellular levels of IFT complex B and A proteins in cell lysates of wild-type and *ift46* cells (Fig. 5, lanes WT and *ift46*). When normalized with tubulin, the levels of complex B proteins IFT20, IFT57, IFT72, and IFT81 were greatly decreased in the mutant cells relative to the wild-type cells. The only complex B protein not reduced in the absence of IFT46 was IFT172, the level of which was the same as or greater than in wild-type

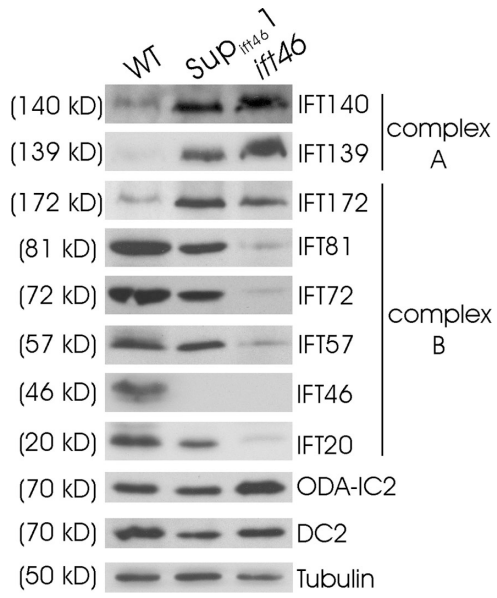

Figure 5. **IFT complex B is unstable in the *ift46* mutant, but stabilized in the partially suppressed strain.** Whole-cell lysates from wild-type cells, $Sup_{ift46}1$ cells, and *ift46* cells were analyzed in Western blots probed with antibodies to several IFT particle proteins, IC2, and DC2. Complex A protein levels are increased in *ift46* compared with wild-type cells. With the exception of IFT172, complex B protein levels are dramatically decreased in *ift46* compared with wild-type cells. The levels of these proteins in $Sup_{ift46}1$ cells are between those in *ift46* and wild-type cells. IFT172 is increased in $Sup_{ift46}1$ cells. Tubulin was used to normalize the loading of the samples. Note that both *ift46* cells and $Sup_{ift46}1$ cells have IC2 and DC2.

cells, depending on the preparation, suggesting that the level of IFT172 is controlled independently from that of the other complex B proteins. In contrast to the decrease in most complex B proteins seen in the *ift46* mutant, the levels of complex A proteins IFT139 and IFT140 were greatly increased in *ift46* cells relative to wild-type cells.

To examine if these differences in protein levels were caused by changes in synthesis or stability, we used real-time PCR to measure transcript levels for several complex A and B proteins in wild-type and *ift46* cells. Transcript levels in the mutant were increased by ~2.8- and ~2.0-fold for complex A proteins IFT140 and IFT139, and by ~1.8- and ~1.6-fold for complex B proteins IFT81 and IFT72, respectively. Therefore, the mutant responds to its defect by increasing the mRNA levels of at least these complex A and B proteins. The increase in complex A proteins in the mutant presumably reflects this increase in mRNA abundance. However, because the levels of most complex B proteins are drastically decreased in the mutant, even though complex B mRNA levels in general appear to be increased, it is likely that these proteins are specifically degraded in the absence of IFT46.

Complex A and B proteins are located in distinct compartments in the basal body region

To determine if the absence of IFT46 and the accompanying large decrease in most other complex B proteins affected the transport of IFT172 or complex A into or out of the flagellum, we used immunofluorescence microscopy to examine *ift46* cells that were double labeled with antibodies to tubulin and IFT172 or IFT139 (Fig. 6 A). In both cases, the IFT particle proteins were concentrated around the basal bodies and in the short flagella. Thus, both proteins are transported into the flagella in the absence of IFT46. Surprisingly, however, the distributions of IFT172 and IFT139 differed from each other in the cell body, with that of IFT172 (Fig. 6 A, a–d) appearing to have almost no overlap with that of IFT139 (Fig. 6 A, e–h), which was more anterior and often concentrated into two distinct lobes.

To clarify whether this difference in distribution was normal or caused by loss of IFT46, wild-type cells were double labeled with antibodies to IFT46 and IFT172 or IFT139. In most cases, IFT46 and IFT172 colocalized precisely with each other in the peribasal body region (Fig. 6 B, a–c), which is consistent with the other evidence that IFT46 is a complex B protein. In contrast, although IFT139 colocalized with IFT46 at the extreme apical end of the cell, the labeling of IFT46 almost always extended more posteriorly than that of IFT139 (Fig. 6 B, d–f). This is the first observation that complex A and B proteins differ in their distribution, and indicates that the complexes, or at least a subset of them, are not physically associated in the cell body. This, together with the results for the *ift46* mutant, also shows that in the absence of IFT46, the colocalization of IFT172 with complex A proteins at the extreme apical end of the cell is lost.

Our observation that IFT172 was transported into the short flagella of the *ift46* mutant (Fig. 6 A) raised the question of whether IFT172 was being transported into the flagella independently of other complex B proteins or in association with incomplete complex B particles, possibly assembled from the small amount of complex B proteins still present in the mutant. To address this question, we used immunofluorescence microscopy to examine the distribution of another complex B protein, IFT57, the levels of which are greatly reduced in the mutant. Like IFT172, the residual IFT57 was transported into the short flagella of the *ift46* mutant (Fig. 6 C). These results support the hypothesis that a small number of incomplete complex B particles assemble from the residual complex B proteins and are capable of being transported into the flagellum in the absence of IFT46. The resulting low level of IFT may account for the ability of the *ift46* cells to assemble their short flagella.

Loss of IFT46 is specifically correlated with loss of the outer dynein arm in a partially suppressed strain

ift46 cells are completely nonmotile. However, on one occasion, swimming cells were observed in an unaerated, stationary phase culture of *ift46* cells. Cells from this culture were cloned, and a partially suppressed strain, $Sup_{ift46}1$, was isolated. $Sup_{ift46}1$ cells are usually nonmotile when grown in M media with aeration, but are stimulated to form flagella of variable length (Fig. 7) and swim with a slow jerky movement in the absence of aeration. The suppressed phenotype is the result of a rare spontaneous mutation that allows transcription of the 3′ end of the IFT46 gene (see next section).

To elucidate the effect of the partial suppressor mutation on IFT46 and other IFT particle proteins, the levels of the

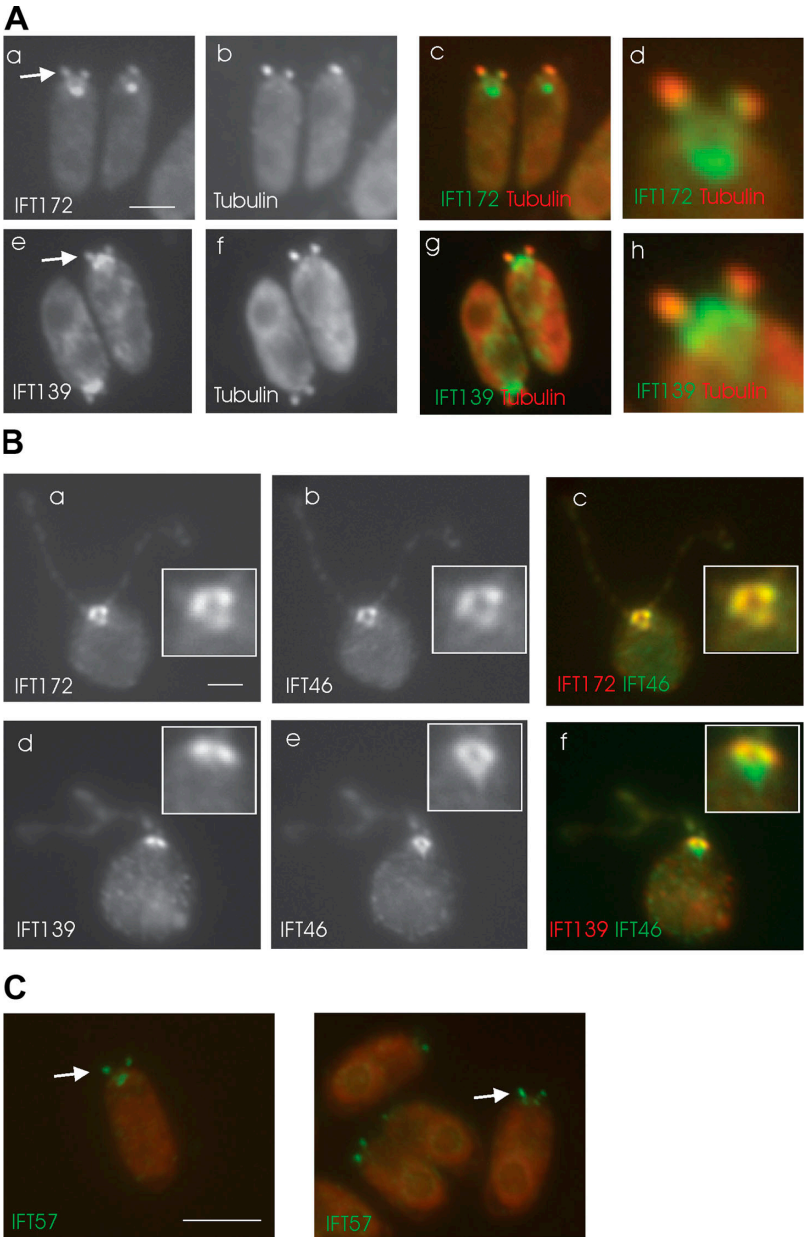

Figure 6. **Complex A and B proteins differ in cellular distribution, and loss of IFT46 affects the cell body localization of IFT172, but not of IFT139.** (A) *ift46* cells were double labeled either with antibodies to IFT172 (a) and tubulin (b) or with antibodies to IFT139 (e) and tubulin (f). c and g are merged images; d and h are enlargements of the flagella and basal body regions. IFT172 and IFT139 are both present in the short flagella (arrows). In the basal body region, IFT139 localizes more anteriorly than IFT172. (B) Wild-type cells were double-labeled either with antibodies to IFT172 (a) and IFT46 (b) or with antibodies to IFT139 (d) and IFT46 (e). The merged images are shown in c and f; the insets show enlargements of the basal body regions. IFT172 usually colocalizes with IFT46. However, IFT139 usually only partially colocalizes with IFT46 in the anterior part of the basal body region. (C) In the absence of IFT46, the remaining complex B proteins are still transported into the flagella. *ift46* cells were labeled with an antibody to IFT57, which is located in flagella (arrows), as well as in the basal body region. Bars, 5 μm.

proteins in stimulated $Sup_{ift46}1$, wild-type, and *ift46* cells were compared by Western blotting. In the $Sup_{ift46}1$ cells, complex B proteins IFT20, IFT57, IFT72, and IFT81 were increased to a level between those of *ift46* and wild-type cells (Fig. 5), whereas the levels of the complex A proteins IFT139 and IFT140 were decreased to a level between those of *ift46* and wild type. Importantly, IFT46 is still undetected in the suppressed strain. This result indicates that the partial suppression of *ift46* involves an increased stability of IFT complex B in the absence of full-length IFT46. It is possible that a C-terminal fragment of IFT46 is expressed in $Sup_{ift46}1$ cells and incorporated into complex B, thereby stabilizing it. Such a fragment would not be detected by our antibody to the N terminus of IFT46.

The slow, jerky swimming of $Sup_{ift46}1$ is typical of outer dynein arm mutants. Therefore, we used immunofluorescence microscopy to check for the presence of outer and inner dynein arms in $Sup_{ift46}1$ flagella. No outer arm dynein was detected using an antibody to the α heavy chain of outer arm dynein (Fig. 7 A, a–i). In contrast, labeling of $Sup_{ift46}1$ flagella by an antibody to inner arm dynein I1 intermediate chain IC138 was normal (Fig. 7 A, j–r). These results show that transport into the flagellum of inner arm dynein I1, but not outer arm dynein, is restored in the suppressed strain.

To determine the extent to which the ultrastructural defects of *ift46* were restored in the partially suppressed strain, $Sup_{ift46}1$ cells and flagella were examined by electron microscopy (Fig. 7 B). The inner arms, radial spokes, and central microtubules were present and appeared normal. However, no outer dynein arms were observed. Therefore, the suppressor strain assembles flagella that lack the outer dynein arm but appear normal in every other way. Western blotting showed that the levels of both outer arm dynein and outer dynein arm docking complex proteins, as

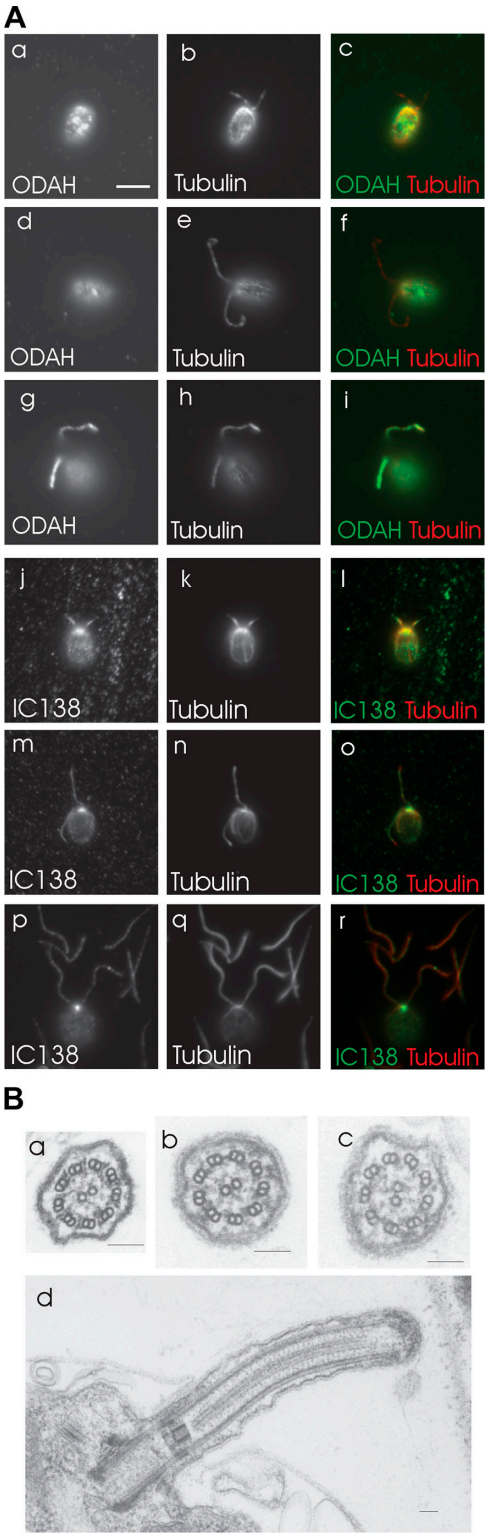

Figure 7. **The partial suppressor of *ift46* has defects in assembly of the outer dynein arm, but not inner dynein arm I1.** (A) Cells were double labeled either with antibodies to outer dynein arm heavy chain α (a, d, and g) and tubulin (b, e, and h), or with antibodies to inner dynein arm intermediate chain IC138 (j, m, and p) and tubulin (k, n, and q). The right column shows the merged images. a–f and j–o are $Sup_{ift46}1$ cells; g–i and p–r are wild-type cells. Note that $Sup_{ift46}1$ cells have flagella of varying lengths. (B) Electron micrographs of wild-type flagella (a) and $Sup_{ift46}1$ flagella (b–d). $Sup_{ift46}1$ flagella lack outer arms, but the axonemal ultrastructure is otherwise normal. Bars: (A) 5 μm; (B) 100 nm.

represented by IC2 and DC2, respectively, were normal in $Sup_{ift46}1$ cells (Fig. 5). Thus, the inability to transport and assemble outer arms in the flagella is not simply caused by an absence of these components from the cell cytoplasm. These results indicate that IFT46 is specifically needed to transport outer dynein arm components into the flagellum. The inner dynein arm and central pair defects observed in the *ift46* mutant are likely attributable to a more general deficiency in IFT caused by the reduced number of complex B particles.

The 3′ end of the *IFT46* gene is transcribed in $Sup_{ift46}1$ cells

Analysis by PCR revealed that the suppressor mutation involved a rearrangement or deletion somewhere in the region between the 3′ end of the inserted *NIT1* gene and the seventh intron of the *IFT46* gene (unpublished data). To determine if this mutation caused a change in the transcription of the *IFT46* gene, wild-type, *ift46*, and $Sup_{ift46}1$ cells were examined by real-time PCR using primer pairs designed to assay for the presence of the 5′ end, middle, and 3′ end of the *IFT46* mRNA (Fig. 8). In wild-type cells, all three regions were detected. In the *ift46* mutant, only the 5′ end was detected, indicating that the 5′ end of the gene is transcribed, but a full-length mRNA is not made. Because our antibody to the N terminus of IFT46 did not detect a product, it appears that the truncated mRNA is not translated into a stable protein. This provides further evidence that *ift46* is a null allele. In $Sup_{ift46}1$ cells, both the 5′ and the 3′ end, but not the middle, were reproducibly detected. Therefore, the suppressor mutation results in transcription, and possibly translation, of the 3′ end of the IFT46 gene. Our antibody would not detect a product containing the C-terminal end of IFT46, but lacking its N-terminal end. However, we can rule out the possibility that the suppressor mutation results in translation of the N-terminal part of IFT46 fused with the C-terminal part of IFT46, because our antibody did not detect any product in $Sup_{ift46}1$ cells. Transcripts encoding the 3′ end of the IFT46 gene were detected in $Sup_{ift46}1$ cells in both the presence and absence of aeration, so the suppressor mutation, not stress, causes transcription of the 3′ end of the gene.

Discussion

The *C. reinhardtii* IFT46 sequence, which is reported for the first time in this study, demonstrates that this protein, like other IFT particle proteins, is highly conserved among ciliated organisms. *C. reinhardtii* IFT46 was previously reported to cosediment with other IFT complex B proteins (Cole et al., 1998). We confirm that IFT46, in both *C. reinhardtii* and mammals, is a complex B protein based on cosedimentation, coimmunolocalization, and coimmunoprecipitation with other complex B, but not complex A, proteins. Our analysis of a *C. reinhardtii ift46* mutant and a suppressed strain of the mutant indicate that IFT46 is necessary for complex B stability and is specifically required to transport outer dynein arm complexes into the flagella.

Our sequencing of *C. reinhardtii* IFT46 also revealed that it is a homologue of *C. elegans* DYF-6 (Starich et al., 1995), the sequence of which was recently reported by Bell et al. (2006).

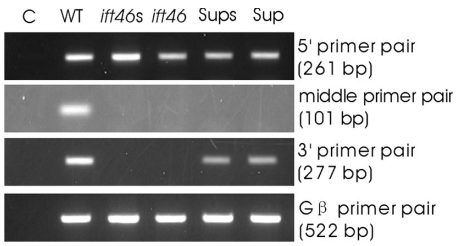

Figure 8. **The 3′ end of the *IFT46* gene is expressed in the suppressor, but not in the *ift46* mutant.** RT-PCR was performed with no added DNA (control, C), or cDNA isolated from wild-type cells (WT), *ift46* cells without aeration (*ift46*s), *ift46* cells with aeration (*ift46*), $Sup_{ift46}1$ cells without aeration (Sups), and $Sup_{ift46}1$ cells with aeration (Sup) using primers designed to amplify transcripts from the 5′, middle, and 3′ regions of the *IFT46* gene. The products were then electrophoresed in 1.5% agarose gels. The results show that the 5′ portion of the *IFT46* gene is transcribed in all the cells. The middle region is not transcribed in either the *ift46* mutant cells or the suppressed cells. The 3′ region is not transcribed in the *ift46* mutant cells, but is transcribed in the suppressed cells. The transcription of the 3′ region of the *IFT46* gene is not dependent on the growth condition. This result implies that the suppression is caused by expression of the 3′ region of the *IFT46* gene.

DYF-6-GFP moves at IFT rates in *C. elegans* sensory cilia and is required for ciliary assembly (Bell et al., 2006), providing independent and complementary evidence that IFT46/DYF-6 is an essential IFT protein. Although both *C. elegans* cilia and mammalian primary cilia lack outer arms, it may be that IFT46 is required for transport of other cargos in these immotile cilia, or simply is needed for complex B assembly, as in *C. reinhardtii*.

IFT46 is important for the stability of complex B

In the *C. reinhardtii* mutant lacking IFT46, levels of both complex A and B mRNAs increased relative to their levels in wild-type cells. This strongly suggests that the genes encoding proteins of both complexes are constitutively induced when the cell cannot assemble flagella. The mutant exhibited a corresponding increase in levels of complex A proteins. However, levels of complex B proteins other than IFT172 decreased in the mutant, suggesting that these proteins are broken down in the absence of IFT46. These results indicate that a) in the absence of IFT46, complex B is unstable; b) stability of complex A proteins is not dependent on the presence of complex B; c) the normal 1:1 stoichiometry between complex A and complex B proteins (Cole et al., 1998) is uncoupled in the absence of IFT46; and d) flagella assembly requires complex B, even in the presence of increased amounts of complex A.

Biochemical analysis (Lucker et al., 2005) has shown that complex B is composed of a 500-kD "core" that includes IFT88, IFT81, IFT74/72, IFT52, IFT46, and IFT27, and four "peripheral" subunits including IFT172, IFT80, IFT57, and IFT20. (The term "core" here refers to a group of proteins that are tightly associated with one another, and has no implication in regard to whether the proteins are or are not exposed on the surface of the IFT particles.) Our finding that IFT46 is required for the stability of all complex B proteins tested except for IFT172 is consistent with this model. In the absence of IFT46, the complex B core is destabilized, leading to degradation of the core subunits, as well as of the peripheral subunits other than IFT172. This is in contrast to the situation when another complex B core protein, IFT88, is disrupted; loss of this protein in an *ift88* mutant had little or no effect on the levels of IFT172 and IFT81, but caused a significant decrease in IFT57 (Pazour et al., 2000). This difference suggests that although IFT46 and IFT88 may both be components of the complex B core, the former is essential for the core's stability, whereas the latter is not. IFT46 is required for the stability of IFT81, and presumably IFT88, but the stability of IFT81 is not dependent on IFT88, in agreement with a model in which IFT81 and IFT88 are in different domains of the core (Lucker et al., 2005), and suggesting that the assembly or stability of both core domains is dependent on IFT46. Because IFT57 is a peripheral protein, it requires either an intact complex B core or direct interaction with IFT88 for its stability.

The *ift46* mutant can form very short flagella with normal outer doublet microtubules, a phenotype that is distinct from that of the other published *C. reinhardtii* IFT complex B–null mutants, *ift88* and *ift52*, which are bald with no axonemal structures extending beyond the transition zone (Pazour et al., 2000; Brazelton et al., 2001). No information is available on how loss of IFT52 affects the other complex B proteins. However, one possible explanation for the difference between the *ift46* and *ift88* mutants is that the residual complex B proteins in both mutants form incomplete complex B particles, and that those formed in the absence of IFT46 have some functionality, whereas those formed in the absence of IFT88 are completely unable to form a flagellum. This could occur if IFT46 served primarily to transport a nonessential axonemal protein, such as outer arm dynein, but IFT88 was necessary for transport of a protein, such as tubulin, which is absolutely necessary for axonemal assembly.

It is of interest that the level of IFT172 in the *ift46* mutant did not show the decrease observed for the other complex B proteins. IFT172 also differs from the other complex B proteins in that it readily dissociates from the rest of the complex B particle during sucrose gradient centrifugation (Fig. 1 D; Cole et al., 1998), and that it interacts with the *C. reinhardtii* microtubule end–binding protein CrEB1 in a manner that does not require association with the other complex B proteins (Pedersen et al., 2005). Thus, IFT172 is unique in that its cellular level is regulated independently of other complex B proteins, that it binds relatively weakly to complex B, and that it can interact with other proteins independently of complex B.

IFT46 is required for transport of outer dynein arms into flagella

In addition to being very short, *ift46* flagella have defects in central pair and dynein arm assembly. Aspects of this phenotype are undoubtedly caused by the greatly reduced amount of complex B in the *ift46* mutant. Because there is not enough IFT machinery to transport a full complement of axonemal proteins, the flagella are short and assembly of specific axonemal structures is affected.

However, our discovery of a suppressor mutation that stabilizes complex B in the absence of full-length IFT46 and

restores flagellar assembly, including assembly of the central pair and the inner dynein arms, but does not restore outer dynein arm assembly, even though outer arm proteins are present in the cytoplasm, strongly argues that IFT46 has a specific role in outer dynein arm transport. This is the first direct evidence that the outer dynein arms require IFT for transport into the flagellum, and the first evidence connecting a specific IFT particle protein with a specific cargo. Because the outer arm components are preassembled in the cytoplasm into complexes as large as 1.2 MD (Fowkes and Mitchell, 1998), it is likely that IFT is needed to move them efficiently into the flagellum and out to the flagellar tip, which is the site of axonemal assembly (Witman, 1975; Johnson and Rosenbaum, 1992).

Further work will be necessary to determine if IFT46 is involved directly in outer arm binding, or if loss of IFT46 causes a conformational change in the IFT particle that eliminates an outer arm binding site at some distance from IFT46. However, the fact that the suppressor mutant has a partially stabilized complex B but still fails to transport outer arms into the flagella strongly supports the first possibility. The first possibility is further supported by the recent finding that the human homologue of ODA16, which is a *C. reinhardtii* flagellar protein that is not a component of dynein but is essential for outer arm transport into the flagellum (Ahmed and Mitchell, 2005), interacts with the mouse homologue of IFT46 in a yeast two-hybrid system, and thus may be an adaptor coupling IFT46 to the outer arm (Ahmed et al., 2006).

Our finding that IFT is involved in transport of outer arm complexes explains a previous observation that antibodies to complex B proteins IFT52 and IFT72 coimmunoprecipitated subunits of the outer dynein arm from a flagellar membrane plus matrix fraction (Qin et al., 2004). An earlier study had reported that inner dynein arms, but not outer dynein arms, required the activity of FLA10, which is one motor subunit of the anterograde IFT motor kinesin-2, for transport into the flagellum (Piperno et al., 1996). There are at least two possible explanations for the difference between these results and our own. First, as discussed by Qin et al. (2004), the earlier studies used a *fla10* temperature-sensitive mutant and observations 45–75 min after shift to the restrictive temperature, which may not have been adequate for complete cessation of FLA10 activity. Second and more interestingly, it is possible that there is more than one kinesin for anterograde IFT in *C. reinhardtii*, as there is in *C. elegans* (Snow et al., 2004). Phylogenetic analysis on complete kinesin repertoires of a diversity of organisms revealed that some kinesin families are specific for ciliated species (Wickstead and Gull, 2006). The *C. reinhardtii* kinesin-2 motor subunits FLA10 and FLA8 and the central pair kinesin KLP1, as well as several novel kinesins, were grouped in these subfamilies; two of the latter (C_250150 in the kinesin-9 family, and C_710026 in the newly proposed kinesin-17 family) were each identified by multiple hits to a single peptide (shared with FLA8) in the *C. reinhardtii* flagellar proteome (Pazour et al., 2005; http://labs.umassmed.edu/chlamyfp/protector_login.php). It is possible that one of the novel kinesins is an IFT anterograde motor, and that it and kinesin-2 transport IFT particles linked to different cargos.

We also observed that the outer dynein arm docking complex, as represented by its DC2 subunit, was transported into the *ift46* mutant flagella. The movement of the docking complex, but not the outer dynein arm, into *ift46* flagella is consistent with previous results that the docking complex is preassembled in the cytoplasm as a distinct complex not associated with the outer arm (Wakabayashi et al., 2001), and that it is transported into the flagellum independently of the outer arm (Takada and Kamiya, 1994; Wirschell et al., 2004). DC2 was coimmunoprecipitated by antibodies to IFT particle proteins (Qin et al., 2004), indicating that it interacts with the IFT machinery and probably is dependent on it for transport into the flagellum. Our results clearly show that the docking complex does not specifically require IFT46 for entry into the flagellum.

Complex A and complex B occur in distinct, but overlapping, compartments in the basal body region

Complexes A and B are associated with each other in large linear assemblages during transport within the flagellum (Qin et al., 2004), and it has been proposed that turnover of IFT particle proteins and motors at the tip of the flagellum involves the dissociation of complex A from complex B, followed by their reassociation before retrograde transport (Pedersen et al., 2006). However, virtually nothing was known about the interactions of the complexes at the base of the flagellum. Our immunofluorescence microscopy observations have revealed different patterns of localization for complex A and complex B proteins in the wild-type cell, with the former localized more apically in the peribasal body region. In contrast, the complex B proteins IFT172 and IFT46 usually colocalized precisely with each other. These results suggest that complex A and complex B separate from each other upon passage from the flagellum into the cytoplasm, are sorted into separate albeit overlapping compartments, and are subsequently reassembled before their transport into the flagellum, in a reversal of the process proposed to occur at the tip of the flagellum. The region of overlap at the apical end of the peribasal body region may correspond to the basal body transition fibers, which are proposed to be docking sites where the IFT particles are assembled or disassembled before entry into the flagellum or cytoplasm, respectively (Deane et al., 2001; Rosenbaum and Witman, 2002). Within the cell body of the *ift46* mutant, the IFT172 in excess over other complex B proteins localizes primarily to the posterior peribasal body region and has little or no overlap with IFT139 in the anterior peribasal body region, indicating that IFT172 does not interact directly with complex A in the cell body.

Our immunofluorescence microscopy studies also showed that both complex A and residual complex B proteins are transported into the short flagella of the *ift46* mutant, indicating that even in the absence of suppression, transport of the IFT complexes into the flagella does not require *ift46*.

Stability of complex B in $Sup_{ift46}1$ cells may be caused by expression of the C-terminus of IFT46

Our analysis of the $Sup_{ift46}1$ cells revealed that they differ from *ift46* cells in that the suppressor mutation causes transcription of the 3′ end of the IFT46 gene. This could come about as a

result of an intragenic mutation that allows transcription of the 3′ end of the IFT46 gene from the *NIT1* promoter present in the vector originally used to generate the *ift46* insertional mutant. Irrespective of the mechanism, the results suggest that the C-terminal portion of IFT46 is expressed, possibly as part of a fusion protein with nitrate reductase (encoded by the *NIT1* gene). This fragment may then be incorporated into complex B, stabilizing it.

Expression of the suppressed phenotype was observed only in $Sup_{ift46}1$ cells grown in the absence of aeration. A possible explanation for this is that under stress conditions (hypoxia), a chaperone is produced that helps stabilize complex B. *ift46* cells do not form flagella in the absence of aeration, so this hypothetical chaperone does not stabilize complex B in the complete absence of IFT46. It may be that a stress-induced chaperone can stabilize complex B in the presence of a C-terminal fragment of IFT46, but not in the absence of the fragment.

Flagella are formed in $Sup_{ift46}1$ cells, but the flagella lack the outer dynein arms. Therefore, if complex B is indeed stabilized by a C-terminal fragment of IFT46 in $Sup_{ift46}1$ cells, this would imply that the N-terminal end of IFT46 is essential for transport of outer arms into the flagellum.

Cells can compensate for defects in IFT complex B

Our identification of a partial suppressor of the *ift46* phenotype is the second report of suppression of the phenotype resulting from disruption of a complex B protein. Brown et al. (2003) identified a spontaneous partial suppressor of a null mutant of IFT52 in *Tetrahymena thermophila*. The *T. thermophila ift52*-null mutant has basal bodies that fail to form flagella or form short flagella that lack the central pair of microtubules, whereas a variable number of cells of the partially suppressed strain had slightly longer flagella, of which ∼13% had a central pair of microtubules, depending on growth conditions. Just as the suppressed phenotype of *C. reinhardtii* $Sup_{ift46}1$ was stimulated by lack of aeration, the suppressed phenotype of the *T. thermophila* strain was stimulated by pericellular hypoxia; suppression of the *T. thermophila* strain was also stimulated by growth at abnormally low temperature. This suppression differed from that which we observed, in that it arose spontaneously with high frequency, whereas ours was a rare event that was observed only once in 2 yr of culturing the cells; however, in both cases, the phenotype was stable during vegetative growth. Therefore, the mechanism of suppression may be similar in both *C. reinhardtii* and *T. thermophila*. In our case, Western blotting showed that the IFT protein levels in the partially suppressed strain were restored to levels between those of wild-type cells and the *ift46* mutant cells, indicating that restoration of the ability to form flagella was caused by stabilization of complex B in the absence of full-length IFT46.

Materials and methods

Cells and culture media

C. reinhardtii strains 137c (*nit1*, *nit2*, *mt+*), CC124 (*nit1*, *nit2*, *mt−*), and S1D2 were obtained from the *Chlamydomonas* Genetics Center (Duke University, Durham, NC). T8a4-11 (*ift46::NIT1*, *nit1*, *pf1*, *mt+*) was generated by K. Kozminski and J. Rosenbaum (Yale University, New Haven, CT) by transforming KK30A3 (*nit1*, *NIT2*, *pf1*, *mt+*) with the plasmid pMN24 linearized with EcoRI. YH6 (*ift46::NIT1*, *PF1*, *mt+*) is an offspring of a cross between T8a4-11 and CC124. $Sup_{ift46}1$ is a spontaneous partial suppressor for YH6. Cells were grown in M (Sager and Granick [1953] medium I altered to have 0.0022 M KH_2PO_4 and 0.00171 M K_2HPO_4), M-N (M medium without nitrogen), or TAP (Gorman and Levine, 1965) media.

Murine IMCD3 cells (CLONTECH Laboratories, Inc.) were grown as described in Follit et al. (2006).

Antibodies

The antibodies used are listed in Table S1 (available at http://www.jcb.org/cgi/content/full/jcb.200608041/DC1). The rabbit antibody to IFT46 was generated against a synthetic peptide corresponding to the protein's N-terminal 19 amino acids (Pocono Rabbit Farm) and affinity purified using the same 19 amino-acid peptide.

C. reinhardtii IFT46 gene cloning

16S IFT particles were purified from *C. reinhardtii* flagella (Cole et al., 1998) and the particle proteins separated by PAGE. A band corresponding to IFT46 was excised and microsequenced. Two peptides, VPRPDTKPDYLGLK and IKPFIPDYIPAVGGIDEFIK, were obtained; these identified the protein C_2130007 predicted by the *C. reinhardtii* genome (v. 2; http://genome.jgi-psf.org/cgi-bin/searchGM?db=chlre2). Several EST clones in Genbank that contain these two peptides in their ORF were used to clone the IFT46 cDNA. A 4.8-kb fragment that contains only the full-length *IFT46* gene was cloned from *C. reinhardtii* genomic DNA after its amplification by PCR with primers IFT46-5 and IFT46-6 (the sequences of all primers are given in Table S2, available at http://www.jcb.org/cgi/content/full/jcb.200608041/DC1) using eLONGase Enzyme Mix (Invitrogen). The sequences of the 5′- and 3′-UTRs of the IFT46 cDNA were verified by sequencing the cloned *IFT46* gene; the sequence of the coding region was verified by sequencing a PCR product from a cDNA library.

IFT46 homologues were identified by searching the translated nr database at http://www.ncbi.nlm.nih.gov/BLAST/. Sequences were analyzed as described in Hou et al. (2004).

DNA and RNA isolation and analysis

DNA was isolated from *C. reinhardtii* as described in Pazour et al. (1998). DNA gel electrophoresis was carried out by standard procedures (Sambrook et al., 1989). Southern blotting was performed using the DIG High Prime DNA Labeling and Detection Starter Kit II (Roche); instead of using the kit's hybridization buffer, we used Church buffer (7% SDS, 1 mM EDTA, and 0.25 M Na_2HPO_4, pH 7.2; Church and Gilbert, 1984) and hybridized it at 65°C.

IFT46 gene induction upon deflagellation was analyzed by real-time PCR, as described in Pazour et al. (2005), using primers IFT46-3 and -4. The ratio of the amount of IFT46 message after deflagellation to that before deflagellation was calculated for each trial. Three independent sets of mRNA were isolated and analyzed three times each.

To measure the mRNA levels of IFT140, IFT81, and IFT72, cDNAs were prepared from cells at the mid-log phase of growth, and quantitated by real-time PCR as described in Pazour et al. (2005) using the primer pairs IFT140F/IFT140R, IFT81F/IFT81R, or IFT72F2/IFT72R2. Two independent sets of mRNA were isolated and analyzed three times each.

To assay transcription of the *IFT46* gene, cDNAs were prepared from wild-type cells and from *ift46* and $Sup_{ift46}1$ cells with or without aeration. Real-time PCR was performed using primer pairs to the 5′ end of the gene (IFT46-11/IFT46-2), middle part of the gene (IFT46-9/IFT46-28), and the 3′ end of the gene (IFT46-3/IFT46-4). Samples were normalized using G protein β subunit (Pazour et al., 2005). The end products were examined on a 1.5% agarose gel. Three independent sets of mRNA were isolated and analyzed three times each.

A collection of insertional mutants having motility defects was screened for a defect in *IFT46* by Southern blotting, using an 864-bp partial cDNA fragment amplified by PCR with primers IFT46-Q1 and IFT46-Q2 as a probe. The mutated region in the *IFT46* gene in the mutant was located by PCR using primer pairs 1 (IFT46-1/IFT46-2), 2 (IFT46-9/IFT46-10), and 3 (IFT46-3/IFT46-4).

Murine IFT46 and Flag-tagged proteins

The open reading frame of MmIFT46 was PCR amplified from mouse testis cDNA using primers mIFT46-1 and -2. The PCR product was digested with BamHI, cloned into the BglII site of pJAF113.1, and called pJAF161.24. pJAF113.1 was derived from p3XFLAG-myc-CMV-26 (Sigma-Aldrich) by

filling in the HindIII site to shift the polylinker by four nucleotides. pJAF161.24 encodes a fusion protein in which the 3× Flag tag is fused to the N-terminal end of IFT46. pJAF146.1 encoding GFP-Flag was constructed by moving the XbaI–EcoRI GFP-containing fragment from pEGFP N2 (CLONTECH Laboratories, Inc.) into pJAF113.1. pJAF134.3 encoding MmIFT20-Flag was described by Follit et al. (2006).

Immunoprecipitations

IMCD3 cells that had been transfected with JAF161.24 (MmIFT46-Flag), pJAF134.3 (MmIFT20-Flag), or pJAF146.1 (GFP-Flag) were lysed in Cell Lytic M (Sigma-Aldrich) containing 0.1% Tween 20 and 0.1% CHAPSO (Bio-Rad Laboratories). After incubation for 10 min at 4°C, the extract was clarified by centrifugation at 18,000 *g* and treated for 10 min with Sepharose-4B beads, which were removed by centrifugation through a Macro Spin Column (Harvard Apparatus). The treated extract was then incubated with anti-Flag M2-Agarose Affinity Gel (Sigma-Aldrich) for 1 h at 4°C. Unbound proteins were removed by washing the beads in Wash Buffer (Sigma-Aldrich) containing 1% Tween 20 and 150 mM NaCl, followed by washes in Wash Buffer alone. Bound proteins were eluted with 200 ng/μl 3× Flag Peptide (Sigma-Aldrich) and analyzed by Western blotting, as described in Pazour et al. (1998).

Protein biochemistry

Preparation of *C. reinhardtii* whole-cell extracts, isolated flagella, and the flagellar membrane plus matrix fraction, as well as PAGE and Western blotting, were performed as described in Pazour et al. (1999). Sucrose gradient analysis was carried out as described by Hou et al. (2004).

Genetic analysis and transformation

T8a4-11 and CC124 gametes were induced to mate by dibutyryl-cAMP and papaverine treatment, and the zygotes were selected by the freeze/thaw method (Pazour et al., 1999; Hou et al., 2004). *ift46* mutant cells were cotransformed (Hou et al., 2004) with linearized plasmid pSP124S (Lumbreras et al., 1998) and the cloned 4.8-kb fragment, which contains only the wild-type *IFT46* gene.

Microscopy

C. reinhardtii cells were fixed in glutaraldehyde for EM (Hoops and Witman, 1983) and processed as described in Wilkerson et al. (1995). *C. reinhardtii* cells were fixed and stained for immunofluorescence microscopy by the alternate protocol of Cole et al. (1998), using Alexa Fluor 488– or 568–conjugated secondary antibodies (Invitrogen); images were acquired at room temperature with an AxioCam camera, AxioVision 3.1 software, and an Axioskop 2 plus microscope equipped with a 100×/1.4 NA oil DIC Plan-Apochromat objective (all from Carl Zeiss MicroImaging, Inc.) and epifluorescence. Mammalian cells were fixed in 2% paraformaldehyde and processed for immunofluorescence microscopy as described by Follit et al. (2006). Images were prepared for final publication using Photoshop 6.0 (Adobe).

Online supplemental material

Table S1 shows the antibodies used in this work. Table S2 shows the primer sequences used in this study. The online version of this article is available at http://www.jcb.org/cgi/content/full/jcb.200608041/DC1.

We thank Dr. W. Dentler for graciously passing on to us the mutant strain T8a4-11; Dr. D. Cole for antibodies to IFT172, IFT139, IFT81, and IFT57; Drs. W. Sale and M. Wirschell for antibodies to IC138; B. Walker for antibodies to *C. reinhardtii* and mouse IFT140; Dr. G. Hendricks of the University of Massachusetts Medical School (UMMS) Electron Microscopy Facility for help with electron microscopy; and Dr. J. Leszyk of the UMMS Proteomic Mass Spectrometry Laboratory for protein sequencing.

This work was supported by National Institutes of Health grants GM60992 (G.J. Pazour), GM14642 (J.L. Rosenbaum), and G30626 (G.B. Witman), and by the Robert W. Booth Fund at the Greater Worcester Community Foundation (G.B. Witman). Core facilities used in this research were supported by grant P30 DK32520.

Submitted: 7 August 2006
Accepted: 22 January 2007

References

Ahmed, N.T., and D.R. Mitchell. 2005. ODA16p, a *Chlamydomonas* flagellar protein needed for dynein assembly. *Mol. Biol. Cell.* 16:5004–5012.

Ahmed, N.T., B. Lucker, D.G. Cole, and D.R. Mitchell. 2006. The *Chlamydomonas ODA16* locus, needed for outer arm dynein assembly, encodes and intraflagellar transport adaptor. 46th Annual Meeting of the American Society for Cell Biology. Abstr. 1612.

Bell, L.R., S. Stone, J. Yochem, J.E. Shaw, and R.K. Herman. 2006. The molecular identities of the *Caenorhabditis elegans* intraflagellar transport genes *dyf-6, daf-10*, and *osm-1. Genetics.* 173:1275–1286.

Brazelton, W.J., C.D. Amundsen, C.D. Silflow, and P.A. Lefebvre. 2001. The *bld1* mutation identifies the *Chlamydomonas osm-6* homolog as a gene required for flagellar assembly. *Curr. Biol.* 11:1591–1594.

Brown, J.M., N.A. Fine, G. Pandiyan, R. Thazhath, and J. Gaertig. 2003. Hypoxia regulates assembly of cilia in suppressors of *Tetrahymena* lacking an intraflagellar transport subunit gene. *Mol. Biol. Cell.* 14:3192–3207.

Church, G.M., and W. Gilbert. 1984. Genomic sequencing. *Proc. Natl. Acad. Sci. USA.* 81:1991–1995.

Cole, D.G. 2003. The intraflagellar transport machinery of *Chlamydomonas reinhardtii. Traffic.* 4:435–442.

Cole, D.G., D.R. Diener, A.L. Himelblau, P.L. Beech, J.C. Fuster, and J.L. Rosenbaum. 1998. *Chlamydomonas* kinesin-II–dependent intraflagellar transport (IFT): IFT particles contain proteins required for ciliary assembly in *Caenorhabditis elegans* sensory neurons. *J. Cell Biol.* 141:993–1008.

Deane, J.A., D.G. Cole, E.S. Seeley, D.R. Diener, and J.L. Rosenbaum. 2001. Localization of intraflagellar transport protein IFT52 identifies basal body transitional fibers as the docking site for IFT particles. *Curr. Biol.* 11:1586–1590.

Follit, J.A., R.A. Tuft, K.E. Fogarty, and G.J. Pazour. 2006. The intraflagellar transport protein IFT20 is associated with the Golgi complex and is required for cilia assembly. *Mol. Biol. Cell.* 17:3781–3792.

Fowkes, M.E., and D.R. Mitchell. 1998. The role of preassembled cytoplasmic complexes in assembly of flagellar dynein subunits. *Mol. Biol. Cell.* 9:2337–2347.

Gorman, D.S., and R.P. Levine. 1965. Cytochrome f and plastocyanin: their sequence in the photosynthetic electron transport chain of *Chlamydomonas reinhardi. Proc. Natl. Acad. Sci. USA.* 54:1665–1669.

Hendrickson, T.W., C.A. Perrone, P. Griffin, K. Wuichet, J. Mueller, P. Yang, M.E. Porter, and W.S. Sale. 2004. IC138 is a WD-repeat dynein intermediate chain required for light chain assembly and regulation of flagellar bending. *Mol. Biol. Cell.* 15:5431–5442.

Hoops, H.J., and G.B. Witman. 1983. Outer doublet heterogeneity reveals structural polarity related to beat direction in *Chlamydomonas* flagella. *J. Cell Biol.* 97:902–908.

Hou, Y., G.J. Pazour, and G.B. Witman. 2004. A dynein light intermediate chain, D1bLIC, is required for retrograde intraflagellar transport. *Mol. Biol. Cell.* 15:4382–4394.

Hou, Y., H. Qin, W.L. Dentler, G.J. Pazour, J.L. Rosenbaum, and G.B. Witman. 2005. Role of IFT46 protein in intraflagellar transport (IFT). 45th Annual Meeting of the American Society for Cell Biology. Abstr. 1017.

Huang, B., M.R. Rifkin, and D.J. Luck. 1977. Temperature-sensitive mutations affecting flagellar assembly and function in *Chlamydomonas reinhardtii. J. Cell Biol.* 72:67–85.

Johnson, K.A., and J.L. Rosenbaum. 1992. Polarity of flagellar assembly in *Chlamydomonas. J. Cell Biol.* 119:1605–1611.

King, S.M., T. Otter, and G.B. Witman. 1985. Characterization of monoclonal antibodies against *Chlamydomonas* flagellar dyneins by high-resolution protein blotting. *Proc. Natl. Acad. Sci. USA.* 82:4717–4721.

Kozminski, K.G., K.A. Johnson, P. Forscher, and J.L. Rosenbaum. 1993. A motility in the eukaryotic flagellum unrelated to flagellar beating. *Proc. Natl. Acad. Sci. USA.* 90:5519–5523.

Kozminski, K.G., P.L. Beech, and J.L. Rosenbaum. 1995. The *Chlamydomonas* kinesin-like protein FLA10 is involved in motility associated with the flagellar membrane. *J. Cell Biol.* 131:1517–1527.

Lucker, B.F., R.H. Behal, H. Qin, L.C. Siron, W.D. Taggart, J.L. Rosenbaum, and D.G. Cole. 2005. Characterization of the intraflagellar transport complex B core: direct interaction of the IFT81 and IFT74/72 subunits. *J. Biol. Chem.* 280:27688–27696.

Lumbreras, V., D.R. Stevens, and S. Purton. 1998. Efficient foreign gene expression in *Chlamydomonas reinhardtii* mediated by an endogenous intron. *Plant J.* 14:441–448.

Pan, J., Q. Wang, and W.J. Snell. 2005. Cilium-generated signaling and cilia-related disorders. *Lab. Invest.* 85:452–463.

Pazour, G.J., B.L. Dickert, and G.B. Witman. 1999. The DHC1b (DHC2) isoform of cytoplasmic dynein is required for flagellar assembly. *J. Cell Biol.* 144:473–481.

Pazour, G.J., C.G. Wilkerson, and G.B. Witman. 1998. A dynein light chain is essential for the retrograde particle movement of intraflagellar transport (IFT). *J. Cell Biol.* 141:979–992.

Pazour, G.J., B.L. Dickert, Y. Vucica, E.S. Seeley, J.L. Rosenbaum, G.B. Witman, and D.G. Cole. 2000. *Chlamydomonas IFT*88 and its mouse homologue, polycystic kidney disease gene *Tg*737, are required for assembly of cilia and flagella. *J. Cell Biol.* 151:709–718.

Pazour, G.J., S.A. Baker, J.A. Deane, D.G. Cole, B.L. Dickert, J.L. Rosenbaum, G.B. Witman, and J.C. Besharse. 2002. The intraflagellar transport protein, IFT88, is essential for vertebrate photoreceptor assembly and maintenance. *J. Cell Biol.* 157:103–113.

Pazour, G.J., N. Agrin, J. Leszyk, and G.B. Witman. 2005. Proteomic analysis of a eukaryotic cilium. *J. Cell Biol.* 170:103–113.

Pedersen, L.B., S. Geimer, R.D. Sloboda, and J.L. Rosenbaum. 2003. The Microtubule plus end-tracking protein EB1 is localized to the flagellar tip and basal bodies in *Chlamydomonas reinhardtii. Curr. Biol.* 13:1969–1974.

Pedersen, L.B., M.S. Miller, S. Geimer, J.M. Leitch, J.L. Rosenbaum, and D.G. Cole. 2005. *Chlamydomonas* IFT172 is encoded by *FLA11*, interacts with CrEB1, and regulates IFT at the flagellar tip. *Curr. Biol.* 15:262–266.

Pedersen, L.B., S. Geimer, and J.L. Rosenbaum. 2006. Dissecting the molecular mechanisms of intraflagellar transport in *Chlamydomonas. Curr. Biol.* 16:450–459.

Perkins, L.A., E.M. Hedgecock, J.N. Thomson, and J.G. Culotti. 1986. Mutant sensory cilia in the nematode *Caenorhabditis elegans. Dev. Biol.* 117:456–487.

Piperno, G., and K. Mead. 1997. Transport of a novel complex in the cytoplasmic matrix of *Chlamydomonas* flagella. *Proc. Natl. Acad. Sci. USA.* 94:4457–4462.

Piperno, G., K. Mead, and S. Henderson. 1996. Inner dynein arms but not outer dynein arms require the activity of kinesin homologue protein KHP1(FLA10) to reach the distal part of flagella in *Chlamydomonas. J. Cell Biol.* 133:371–379.

Porter, M.E., R. Bower, J.A. Knott, P. Byrd, and W. Dentler. 1999. Cytoplasmic dynein heavy chain 1b is required for flagellar assembly in *Chlamydomonas. Mol. Biol. Cell.* 10:693–712.

Qin, H., D.R. Diener, S. Geimer, D.G. Cole, and J.L. Rosenbaum. 2004. Intraflagellar transport (IFT) cargo: IFT transports flagellar precursors to the tip and turnover products to the cell body. *J. Cell Biol.* 164:255–266.

Qin, H., D.T. Burnette, Y.K. Bae, P. Forscher, M.M. Barr, and J.L. Rosenbaum. 2005. Intraflagellar transport is required for the vectorial movement of TRPV channels in the ciliary membrane. *Curr. Biol.* 15:1695–1699.

Rosenbaum, J.L., and G.B. Witman. 2002. Intraflagellar transport. *Nat. Rev. Mol. Cell Biol.* 3:813–825.

Sager, R., and S. Granick. 1953. Nutritional studies with *Chlamydomonas reinhardi. Ann. N. Y. Acad. Sci.* 56:831–838.

Sambrook, J., E.F. Fritsch, and T. Maniatis. 1989. Molecular Cloning: A Laboratory Manual. Cold Spring Harbor Laboratory, Cold Spring Harbor, NY.

Scholey, J.M. 2003. Intraflagellar transport. *Annu. Rev. Cell Dev. Biol.* 19:423–443.

Signor, D., K.P. Wedaman, J.T. Orozco, N.D. Dwyer, C.I. Bargmann, L.S. Rose, and J.M. Scholey. 1999. Role of a class DHC1b dynein in retrograde transport of IFT motors and IFT raft particles along cilia, but not dendrites, in chemosensory neurons of living *Caenorhabditis elegans. J. Cell Biol.* 147:519–530.

Silflow, C.D., and J.L. Rosenbaum. 1981. Multiple alpha- and beta-tubulin genes in *Chlamydomonas* and regulation of tubulin mRNA levels after deflagellation. *Cell.* 24:81–88.

Snow, J.J., G. Ou, A.L. Gunnarson, M.R. Walker, H.M. Zhou, I. Brust-Mascher, and J.M. Scholey. 2004. Two anterograde intraflagellar transport motors cooperate to build sensory cilia on *C. elegans* neurons. *Nat. Cell Biol.* 6:1109–1113.

Starich, T.A., R.K. Herman, C.K. Kari, W.H. Yeh, W.S. Schackwitz, M.W. Schuyler, J. Collet, J.H. Thomas, and D.L. Riddle. 1995. Mutations affecting the chemosensory neurons of *Caenorhabditis elegans. Genetics.* 139:171–188.

Takada, S., and R. Kamiya. 1994. Functional reconstitution of *Chlamydomonas* outer dynein arms from α-β and γ subunits: requirement of a third factor. *J. Cell Biol.* 126:737–745.

Tuffanelli, D.L., F. McKeon, D.M. Kleinsmith, T.K. Burnham, and M. Kirschner. 1983. Anticentromere and anticentriole antibodies in the scleroderma spectrum. *Arch. Dermatol.* 119:560–566.

Wang, Q., J. Pan, and W.J. Snell. 2006. Intraflagellar transport particles participate directly in cilium-generated signaling in *Chlamydomonas. Cell.* 125:549–562.

Wakabayashi, K., S. Takada, G.B. Witman, and R. Kamiya. 2001. Transport and arrangement of the outer-dynein-arm docking complex in the flagella of *Chlamydomonas* mutants that lack outer dynein arms. *Cell Motil. Cytoskeleton.* 48:277–286.

Wickstead, B., and K. Gull. 2006. A "holistic" kinesin phylogeny reveals new kinesin families and predicts protein functions. *Mol. Biol. Cell.* 17:1734–1743.

Wilkerson, C.G., S.M. King, A. Koutoulis, G.J. Pazour, and G.B. Witman. 1995. The 78,000 *M*(r) intermediate chain of *Chlamydomonas* outer arm dynein is a WD-repeat protein required for arm assembly. *J. Cell Biol.* 129:169–178.

Wirschell, M., G. Pazour, A. Yoda, M. Hirono, R. Kamiya, and G.B. Witman. 2004. Oda5p, a novel axonemal protein required for assembly of the outer dynein arm and an associated adenylate kinase. *Mol. Biol. Cell.* 15:2729–2741.

Witman, G.B. 1975. The site of *in vivo* assembly of flagellar microtubules. *Ann. N. Y. Acad. Sci.* 253:178–191.